# Proteome changes upon in ovo stimulation with *Lactobacillus* synbiotic in chicken liver

Aleksandra Dunislawska,[*,1,2] Agnieszka Herosimczyk,[†,1] Malgorzata Ozgo,[†] Adam Lepczynski,[†] Andrzej Krzysztof Ciechanowicz,[‡] Marek Bednarczyk,[*] and Maria Siwek[*]

[*]*Department of Animal Biotechnology and Genetics, Bydgoszcz University of Science and Technology, Mazowiecka 28, Bydgoszcz 85-084, Poland;* [†]*Department of Physiology, Cytobiology and Proteomics, West Pomeraninan University of Technology, Janickiego 29, Szczecin 71-270, Poland; and* [‡]*Department of Regenerative Medicine, Centre for Preclinical Research and Technology, Medical University of Warsaw, Zwirki and Wigury 61, Warsaw 02-091, Poland*

**ABSTRACT** The liver, as the main metabolic organ, plays a key role in many vital processes, including nutrient metabolism, fat digestion, blood protein synthesis, and endocrine management. As one of the immune organs, it has a remarkable ability to adequately activate the immune cells in response to metabolic signals. The anatomy of the liver ensures its close interaction with the gut so that nutrients and gut microbiota contribute to normal metabolism. In chickens, the intestinal microbiota plays an important role in supporting health and improving production parameters. The most effective method of stimulating the microbiota is to administer an appropriate bioactive compound during embryonic development. In ovo stimulation on d 12 of egg incubation involves the delivery of the substance into the air chamber. The aim of the study was to analyze the changes at the protein level after in ovo administration of the synbiotic on d 12 of egg incubation. Our study is the first to conduct a proteome analysis in liver after the administration of a *Lactobacillus* synbiotic in ovo. Eggs of broiler chickens were injected with a synbiotic—*Lactobacillus plantarum* with raffinose family oligosaccharides (**RFO**). On d 21 posthatching liver was collected. We performed analyses based on two-dimensional electrophoresis, matrix-assisted laser desorption/ionization (**MALDI**) time-of-flight, and MALDI Fourier-transform ion cyclotron resonance to obtain a global view of the hepatic proteome changes in response to in ovo injection. A representative pattern of significantly altered liver proteins was observed after stimulation with the synbiotic. A total of 16 protein spots were differentially expressed, with 5 downregulated and 11 upregulated spots. We conclude that the in ovo synbiotic treatment had the potential to accelerate the major energy-yielding metabolic pathways in the liver of adult broilers.

**Key words:** in ovo technology, liver, prebiotic, probiotic, proteome

2021 Poultry Science 100:101449
https://doi.org/10.1016/j.psj.2021.101449

## INTRODUCTION

The liver plays an important role as an endocrine and exocrine gland and is involved in a wide range of metabolic and homeostatic functions. It is also responsible for most of the synthesis, metabolism, excretion, and detoxification processes. The liver removes harmful substances from the blood, stores vitamins and iron, and reserves excess glucose as fat and converts it back into functional sugar in times of deficiency (Szabo, 2015). Furthermore, it is one of the immune organs and has a remarkable ability to activate the immune cells in response to gut- or pathogen-derived metabolic signals. It also affects the immune status of the organism by removing bacteria from the bloodstream (Racanelli and Rehermann, 2006). The specialized macrophages located in the liver can destroy the blood cells and pathogens that enter through the portal vein. The anatomy of the liver ensures its close interaction with the gut (gut−liver axis) so that nutrients and gut microbiota contribute to normal metabolism (Szabo, 2015; Tripathi et al., 2018).

The gut microbiota plays a key role in keeping chickens in good health and improving their production parameters. They are a complex population of microorganisms, the natural habitat of which is the mucosa of the host organism (Patterson and Burkholder, 2003). In young animals, the intestinal microbiota shapes the structure of the intestines and the development of the



Received March 3, 2021.
Accepted August 26, 2021.

[1]These authors contributed equally to this work.
[2]Corresponding author: aleksandra.dunislawska@pbs.edu.pl

immune system. In adults, they play an important role in maintaining normal health as well as regulating the processes of digestion, absorption, and metabolism of nutrients (Hajati and Rezaei, 2010).

The composition of the intestinal microbiota can be modified if the process is carried out early in life. This modification has an impact on the metabolism of the organism later during the development (Bäckhed, 2011). The appropriate composition of the intestinal microbiota and communication between the microbiome and the host are conditioned by the proper development of tissues, especially the immune tissues (Tlaskalová-Hogenová et al., 2011). In ovo technology allows bioactive substances to be delivered during embryonic development and intestinal microbiota to be modified before hatching (Villaluenga et al., 2004). The administration of synbiotics to the air chamber of an egg on d 12 of incubation has long-term effects in response to stimulation and leads to changes in the composition of the gut microbiota. This, in turn, indirectly affects the expression levels of genes involved in many metabolic and immune pathways (Siwek et al., 2018). The essential element of in ovo stimulation is the administration of a specific bioactive containing a prebiotic that stimulates the native intestinal microbiota of the developing embryo and a probiotic, a strain with beneficial properties, which enriches the host's microbiota (Bednarczyk et al., 2016). The 2 bioactives (prebiotic and probiotic) combined together create a synbiotic. The synbiotic proposed in this study exhibits the notable feature of synergism with the components of the host (Dunislawska et al., 2017). The prebiotic and probiotic act independently in the digestive system of the host. The prebiotic component stimulates the development of microbiota and improves the microbiological balance in the intestines of the host (Fuller, 1989), while beneficial microorganisms from the probiotic component colonize its digestive system (Gibson and Roberfroid, 1995).

Early stimulation of the intestinal microbiota by in ovo administration of synbiotic on d 12 has numerous advantages. First, we showed that the administration of the *Lactobacillus* synbiotic influences gene expression at the mRNA level in the liver of broiler chickens, activating mainly metabolism- and development-related pathways (Dunislawska et al., 2019). Second, we proved that the negative regulation of gene expression in the liver occurring after in ovo administration of synbiotics is of epigenetic nature and is closely related to DNA methylation (Dunislawska et al., 2020) and miRNA activity (Sikorska et al., 2021). The research hypothesis of this study assumes that the synbiotic based on *Lactobacillus plantarum* and raffinose family oligosaccharides (**RFO**) administered in ovo on d 12 of egg incubation causes changes in the expression of proteins in the liver. The main aim of this study was to show the changes occurring at the protein level and indicate the pathways activated in the liver after in ovo delivery of synbiotic into the egg chamber. The study complements previous gene expression analyses. To the best of our knowledge, it is also the first to report changes in the liver proteome upon in ovo stimulation.

## MATERIALS AND METHODS

### *Chicken Rearing and in Ovo Injection*

In all, 5,850 Cobb 500 FF eggs (Cobb Vantress B.V., Boxmeer, Holland) were incubated in a commercial hatchery (Drobex-Agro, Solec Kujawski, Poland). Eggs were incubated in Petersime incubator (vision version, Petersime NV, Zulte, Belgium) at 37.8°C and relative humidity between 61 and 63%. On d 12 of incubation, after candling, eggs were randomly distributed between experimental and control groups. The eggs in the control group (C) were injected with 0.2 mL of physiological saline (0.9%) whereas those in the experimental group (S) received 0.2 mL of the synbiotic administered in ovo into the egg chamber. The synbiotic consisted of RFO (2 mg/egg) isolated from seeds of lupin *Lupinus luteus* L. cv. Lord (Ciesiolka et al., 2005) and *Lactobacillus plantarum* IBB3036 ($10^5$ bacteria cfu/egg). After injection, holes in the eggs were sealed with natural glue and incubation was continued. The method of synbiotic selection, dose optimization, and in ovo synbiotic injection has been described by Dunislawska et al. (2017). After hatching, the birds were sexed and the roosters were reared. As reported in the study of Dunislawska et al. (2017), hatchability was 91.9% in the control group and 91.6% in the synbiotic group. The main experiment was conducted in a commercial farm (Piast, Olszowa, Experimental Unit 0161, Poland). First, 160 roosters were randomly chosen (80 individuals per group) and split into 8 replicate pens (10 individuals per pen). Eight replications per each experimental group were reared in a chicken house to evaluate the effect of the administered synbiotic on growth performance (Dunislawska et al., 2017). Chickens had ad libitum access to fresh drinking water and were fed from d 1 of life. A starter diet was fed during d 1 to 10, and a grower diet was fed from d 11 to d 21. Table 1 presents the composition of the diets.

Randomly selected individuals from the experimental group and control group were sacrificed on d 21 by cervical dislocation. The tissues intended for analysis were collected on d 21 and were chosen on the basis of the gene expression analysis that was carried out on d 7, 14, 21, and 42 (Dunislawska et al., 2017). Liver samples were collected from eight individuals per group, and were frozen and stored for protein isolation. The production data of this experiment are presented in the paper of Dunislawska et al. (2017). The feed intake was 4,940 g in the control group and 4,898 g in the synbiotic group throughout the rearing period. No differences were found in feed conversion efficiency between the groups. The body weight gain during the entire rearing period was 3,105 g in the control group and 3,070 g in the synbiotic group. Mortality in the synbiotic group (1.17%) was lower compared to the control group (1.83%). Animal use for experiments was approved by the Local Ethical Committee for Animal Experimentation, University of Science and Technology, Bydgoszcz, Poland (Approval No. 36/2012 on 12 July 2012).

**Table 1.** Chemical composition and nutritive value of commercial feeds used for COBB 500 FF chickens (based on Tavaniello et al. 2019).

| Items (% unless noted) | Starter (d 1−d 10) | Grower (d 11−d 21) |
|---|---|---|
| Ingredients | | |
| Maize (7.75% CP) | 61.16 | 65.99 |
| Soybean meal (47.75% CP) | 33.09 | 28.16 |
| Soybean oil | 1.75 | 2.06 |
| Limestone flour | 1.10 | 0.98 |
| NaCl | 0.20 | 0.20 |
| Dicalcium phosphate | 1.605 | 1.504 |
| Vitamin-mineral premix, supplied per kg of diet | * | ** |
| Chemical analysis | | |
| Dry Matter | 88.87 | 88.94 |
| Crude protein | 21.00 | 19.00 |
| Lipid | 4.61 | 4.99 |
| Crude fiber | 2.69 | 2.63 |
| Ash | 5.82 | 5.40 |
| Calculated analysis | | |
| Metabolizable energy, MJ/kg of diet | 12.72 | 13.00 |
| Lysine | 1.32 | 1.19 |
| Methionine | 0.65 | 0.58 |
| Methionine+cysteine | 0.98 | 0.89 |
| Threonine | 0.86 | 0.78 |
| Tyrosine | 0.25 | 0.22 |
| Calcium | 0.90 | 0.84 |
| Available P | 0.71 | 0.68 |
| Sodium | 0.16 | 0.16 |
| Salt | 0.35 | 0.35 |
| Potassium | 0.93 | 0.83 |

*Vitamin A 13,000 IU; vitamin D3 5,000 IU; vitamin E 80 mg; vitamin B1 3 mg; vitamin B2 9 mg; vitamin B6 4 mg; vitamin B12 20 $\mu$g; vitamin K 3 mg; biotin 0.15 mg; Ca pantothenate 15 mg; nicotinic acid 60 mg; folic acid 2 mg; cholinechloride 0.50 mg; lysine 2812 mg; methionine 3405 mg; threonine 745 mg; Ca iodate 1 mg; Se 0.35 mg; Fe 40 mg; Mo 0.50 mg; Mn 100 mg; Cu 15 mg; Zn, 100 mg.

**Vitamin A 10,000 IU; vitamin D3 5,000 IU; vitamin E 50 mg; vitamin B1 2 mg; vitamin B2 8 mg; vitamin B6, 3 mg; vitamin B12, 15 $\mu$g; vitamin K, 3 mg; biotin, 0.12 mg; Ca pantothenate 12 mg; nicotinic acid 50 mg; folic acid 2 mg; cholinechloride 0.40 mg; lysine 2,831 mg; methionine 3,018 mg; threonine 726 mg; Ca iodate 1 mg; Se 0.35 mg; Fe 40 mg; Mo 0.50 mg; Mn 100 mg; Cu 15 mg; Zn 100 mg.

## Protein Extract Preparation

Liver samples (0.1 g) were homogenized in 1,000 $\mu$L of a lysis buffer containing 7 M urea, 2 M thiourea, 4% (w/v) CHAPS, 1% (w/v) DTT, 2% (v/v) Biolyte, 1% (v/v) protease inhibitor cocktail, and 0.1% (v/v) nuclease at a frequency of 20,000 Hz for 60 min using a mechanical homogenizer (Tissue Lyser, Qiagen GmbH, Hilden, Germany). Insoluble tissue debris was removed by centrifugation (20,800 g for 15 min at 4°C), and the supernatant containing the solubilized liver proteins was collected and used for two-dimensional electrophoresis (**2-DE**) analysis.

## Two-Dimensional Electrophoresis

The 2-DE analysis has been previously described by Herosimczyk et al. (2018, 2020). Briefly, isoelectric focusing (**IEF**) was performed using 24-cm, pH 4−7 ReadyStrip IPG Strips (Bio-Rad, Hercules, CA; 24 cm). The liver protein samples were diluted in a lysis buffer (7 M urea, 2 M thiourea, 4% (w/v) CHAPS, 1% (w/v) DTT, and 2% (v/v) Biolyte) with the final volume of 650 $\mu$L containing 1,000 $\mu$g of proteins. The IPG strips were first subjected to passive in-gel rehydration (0 V, 20°C, and 6 h) followed by active rehydration (50 V, 20°C, and 12 h). IEF was then carried out at 20°C with Protean IEF Cell (Bio-Rad, Hercules, CA), using the following voltage program: 1) a rapid ramp to 250 V over 250 Vh, followed by 2) a rapid ramp to 500 V over 500 Vh, 3) a rapid ramp to 1,000 V over 1,000 Vh, 4) a linear ramp to 5,000 V over 2 h, and finally 5) a rapid ramp to 5,000 V until all the IPG strips reached 90,000 Vh. Subsequently, the IPG strips were prepared for the second dimension (sodium dodecyl sulfate-polyacrylamide gel electrophoresis [**SDS-PAGE**]). For this purpose, they were first equilibrated in a buffer containing 6 M urea, 0.5 M Tris/HCl (pH 6.8), 2% (w/v) SDS, 30% (w/v) glycerol, and 1% (w/v) DTT for 15 min to reduce the sulfhydryl groups and then incubated in a buffer composed of 6 M urea, 0.5 M Tris/HCl (pH 6.8), 2% (w/v) SDS, 30% (w/v) glycerol, and 2.5% (w/v) iodoacetamide for 20 min to alkylate the sulfhydryl groups. The SDS-PAGE was run on 12% SDS polyacrylamide gel at 40 V for 3 h and then at 100 V for 15 h at 15°C in a Protean Plus Dodeca Cell electrophoretic chamber (Bio-Rad, Hercules, CA). The Precision Plus Protein Standard Plugs (Bio-Rad, Hercules, CA) were placed on the gel to estimate the molecular weights of the analyzed proteins. After the second dimension, the gels were stained with colloidal Coomassie Brilliant Blue G-250 according to a previously described method (Pink et al., 2010).

## Acquisition of 2-D Images and Data Analysis

The 2-D gel image analysis was performed as previously described by Herosimczyk et al. (2018, 2020). For each group (control and experimental), 8 biological replicates were run. Sixteen samples were separated twice using 2-DE, resulting in a total of 32 gels. All the bioinformatic and statistical analyses were performed using PDQuest Analysis software version 8.0.1 Advanced (Bio-Rad, Hercules, CA). The gel images from the control and synbiotic groups were aligned, and a match set was created. The match set comprised each spot present on any of the gels included in the specific analyzed group. Thus, for each group (C and S), an individual match set was created. Next, all the match sets from the 2 groups were merged and used as a master gel. The master gel was then used for automatic spot detection and spot boundary identification. The images were manually edited to confirm spot detection and matching. Subsequently, the spots of poor quality (too faint) or artifacts (those that were not really spots but speckles or saturated spots), or spots present only on 4 gels were excluded from the experiment. This allowed detecting approximately 420 to 510 spots on each 2-D gel. The spots were normalized according to the local regression model (**LOESS**) which corrects for any possible differences in staining efficiency occurring for different concentrations in the resolved protein sample. The degree of

difference between the protein groups was expressed as an average ratio. To measure the variability within the groups, the coefficient of variation (**CV**) was calculated. Every spot on a gel was quantified, experimental group-specific averages for each spot were determined, and finally statistical analysis was performed to identify the differences in the proteins differing between the control and in ovo synbiotic-treated groups. For the statistical analysis, a paired two-tailed Student's $t$ test (C vs. S) was performed to determine the differences in the average protein abundance between the gels, considering $P < 0.05$ as significant. Liver protein spots that were significantly ($P < 0.01$ or $P < 0.05$) larger or smaller were considered as differentially expressed and presented as the final result of the experiment. The average ratio values for the liver proteins are presented in Table 2 (C vs. S). Based on the standard 2-D markers, the experimental isoelectric point (**pI**) and molecular weight (kDa) values were computed for each identified protein spot.

### Mass Spectrometry and Bioinformatic Data Analysis

Spots representing differentially expressed proteins were excised from the gels (3 replicates), and the resulting gel pieces were processed as previously described by Ozgo et al. (2019). In this study, 2 different matrix-assisted laser desorption/ionization time-of-flight mass spectrometry (**MALDI−TOF MS**) instruments were used to identify the protein spots—Microflex MALDI-TOF mass spectrometer (Bruker Daltonics, Germany) and 7T SolariX 2xR MALDI Fourier-transform ion cyclotron resonance (FT-ICR) mass spectrometer (Bruker Daltonics). After tryptic digestion, 1 $\mu$L of the peptides was placed on a MALDI-MSP AnchorChip 600/96 plate (Bruker Daltonics) and an MTP ANCHORCHIP # 384 BC (Bruker Daltonics) for analysis by these spectrometers.

At first, the peptide mass fingerprint (**PMF**) spectra were obtained using the Microflex MALDI-TOF mass spectrometer as previously described by Ozgo et al. (2019). Subsequently, spots that were not successfully identified with this mass spectrometer were further subjected to analysis using 7T SolariX 2xR MALDI FT-ICR mass spectrometer equipped with a dual ESI-MALDI source and smartbeam II 1-kHz, 355-nm solid-state Nd:YAG laser focused to a diameter of ~25 $\mu$m. The mass spectra were collected in the positive mode with 1,000 laser shots from each spot. The internal mass calibration was carried out through lock mass calibration on a known $m/z$ and an external Sodium Formic Acid (NaFA) cluster calibrant. Data were acquired with ftControl software and analyzed using DataAnalysis software (Bruker Daltonics).

All PMF data, regardless of the MALDI−TOF mass spectrometer used, were compared to vertebrate databases (SWISS-PROT; http://us.expasy.org/uniprot/ and NCBI; http://www.ncbi.nlm.nih.gov/) using MASCOT search engine (http://www.matrixscience.com/) in ProteinScape 4.2 software (Bruker Daltonics). The searches were limited to the following criteria: trypsin as an enzyme, carbamidomethylation as a fixed modification, and oxidation (M) as a variable modification were set for the Microflex MALDI-TOF MS data; and deamidation (NQ), oxidation (M), and Gln→pyro-Glu (N-term Q) were set as variable modifications for the 7T SolariX 2xR MRMS data. The error tolerance was set from 50 to 150 ppm, and the number of allowed missed cleavage sites was set to 2. Protein identification was approved when the protein score was significant ($P < 0.05$) with at least eight matching peptides and 20% sequence coverage.

### Statistical Analysis

The differentially expressed liver proteins were further categorized according to their biological functions and known pathways using STRING v11 (Szklarczyk et al., 2011). The subcellular localization of proteins was defined according to the UniProtKB database (http://www.uniprot.org). Statistical analysis of the data on protein spot expression comparing the control and in ovo synbiotic-treated groups was performed using Student's $t$ test, included in PDQuest software (Bio-Rad, Hercules, CA), with $P < 0.05$ considered as significant.

## RESULTS

In the present study, we performed 2-DE, MALDI TOF, and MALDI FT-ICR analyses to obtain a global view of the hepatic proteome changes in adult broilers occurring in response to in ovo injection of a synbiotic—*L. plantarum* with RFO. Figure 1 shows a representative 2-D pattern of significantly altered liver proteins after in ovo synbiotic delivery in comparison to C group. A total of 16 protein spots were differentially expressed in the synbiotic group, with 5 downregulated and 11 upregulated spots. Spot No. 5, identified as bifunctional glutamate/proline-tRNA ligase, was the most underexpressed spot (0.44-fold decrease), whereas keratin, type I cytoskeletal 42 (representing spot No. 4) displayed the highest expression (2.26-fold increase). The 2-D gel analysis showed an average CV (or CV%) of 37.55 for the control group and 31.71 for the synbiotic group. Table 2 lists the differentially regulated liver proteins with details of the 2-DE, MALDI-TOF, and MALDI MRMS coordinates for each spot. The majority of these proteins (62%) were identified based on *Gallus gallus* identities. In addition, all proteins of interest were categorized according to their subcellular localization as well as biological processes on the basis of UniProtKB database. Subcellular distribution analysis revealed that the largest proportion of the protein class was constituted by the mitochondrial proteins (44%), suggesting that mitochondrial functions are primarily affected in response to in ovo synbiotic administration. This was followed by cytoskeletal (25%) and cytoplasmic proteins (25%), and the remaining 6% were accounted for by the proteins of

**Table 2.** Summary of the differentially expressed protein spots identified by MALDI-TOF MS and MALDI FT-ICR MS analysis in broiler chicken liver after in ovo injection of synbiotic – *Lactobacillus plantarum* with RFO (S) compared to the control (C) group. Spot number correspond to those in Figure 1.

| Spot no. | Accession no. UniProt/NCBI | Protein name (short protein name or gene name) | Ratio S/C[1] | SC[2] (%)/ MS[3] | MVM[4] | Theo. pI/Mw[5] | Exp. pI/Mw[6] | SL[7] | Taxonomy |
|---|---|---|---|---|---|---|---|---|---|
| Chaperone proteins | | | | | | | | | |
| 1 | KFW95982 | Heat shock 70 kDa protein 8 (HSP70)[A] | 0.63** | 49/165 | 18 | 6.18/48.91 | 4.90/98.50 | CP | *Phalacrocorax carbo* |
| 8 | XP_426159 | Reticulocalbin-1 (RCN1)[A] | 1.42* | 34/85 | 9 | 4.55/37.91 | 3.60/62.10 | ER | *Gallus gallus* |
| 15 | P84173 | Prohibitin (PHB)[B] | 0.73* | 55/133 | 8 | 5.57/29.93 | 5.10/47.30 | MT | *Gallus gallus* |
| Metabolism-related proteins | | | | | | | | | |
| 2 | XP_417933 | Dihydrolipoyllysine-residue acetyltransferase component of pyruvate dehydrogenase complex, mitochondrial (PDCE2)[A] | 1.78* | 28/88 | 10 | 7.97/66.99 | 5.00/112.40 | MT | *Gallus gallus* |
| 5 | Q7SIA2 | Bifunctional glutamate/proline-tRNA ligase (EPRS1)[B] | 0.44* | 31/79 | 35 | 6.78/17.15 | 5.20/89.40 | CP | *Cricetulus griseus* |
| 6 | XP_424298 | ATP synthase subunit beta, mitochondrial precursor (ATP5B)[A] | 1.48* | 60/209 | 20 | 5.44/56.65 | 4.20/79.40 | MT | *Gallus gallus* |
| 7 | P00368 | Glutamate dehydrogenase 1, mitochondrial (GDH 1)[A] | 0.60* | 22/63 | 10 | 8.48/56.05 | 5.20/78.00 | MT | *Gallus gallus* |
| 12 | XP_421886 | NADH dehydrogenase [ubiquinone] 1 alpha subcomplex subunit 10, mitochondrial (NDUFA10)[A] | 1.54* | 37/111 | 10 | 6.15/41.63 | 4.90/60.40 | MT | *Gallus gallus* |
| 14 | XP_015148593 | Pyruvate dehydrogenase E1 component subunit beta, mitochondrial (PDHE1-B)[A] | 1.83* | 35/94 | 9 | 5.95/39.31 | 4.30/45.90 | MT | *Gallus gallus* |
| Cytoskeletal-related proteins | | | | | | | | | |
| 4 | XP_548099 | Keratin, type I cytoskeletal 42 (CK-42)[B] | 2.26* | 63/87 | 50 | 5.19/54.39 | 4.60/91.90 | CS | *Canis lupus familiaris* |
| 9 | P84336 | Actin, cytoplasmic 1 (ACTB)[B] | 2.09** | 65/63 | 21 | 5.30/42.17 | 4.20/60.90 | CS | *Camelus dromedarius* |
| 10 | P84336 | Actin, cytoplasmic 1 (ACTB)[B] | 2.06* | 85/67 | 36 | 5.30/42.17 | 4.30/59.30 | CS | *Camelus dromedarius* |
| 13 | XP_015132753 | Tropomyosin beta chain isoform X7 (TPM2)[A] | 1.66* | 41/138 | 14 | 4.65/28.53 | 3.30/45.10 | CS | *Gallus gallus* |
| 16 | XP_015151889 | Microtubule-associated protein RP/EB family member 1 isoform X1 (MAPRE1)[A] | 1.59* | 42/91 | 9 | 5.04/29.67 | 4.30/39.10 | CS | *Gallus gallus* |
| Transport proteins | | | | | | | | | |
| 3 | P19121 | Serum albumin (ALB)[B] | 0.56** | 78/66 | 52 | 5.51/71.87 | 4.70/95.10 | CP | *Gallus gallus* |
| 11 | Q86VD7 | Mitochondrial coenzyme A transporter SLC25A42[B] | 2.22* | 73/63 | 28 | 10.08/35.44 | 4.90/62.80 | MT | *Homo sapiens* |

Values marked with * differ significantly at $P < 0.05$. Values marked with ** differ significantly at $P < 0.01$.
Proteins marked with [A] were identified using the Microflex MALDI-TOF mass spectrometer (Bruker Daltonics, Germany).
Proteins marked with [B] were identified the 7T solariX MALDI FT-ICR mass spectrometer (SolariX 2xR, Bruker Daltonics, Germany).
Abbreviations: CP, cytoplasm; CS, cytoskeleton; ER, endoplasmic reticulum; M, mitochondrion.
[1]Ratio of protein spot expression found in the liver of broiler chicken after in ovo injection of synbiotic – *Lactobacillus plantarum* with RFO (S) when compared with the control (C) group.
[2]The percentage of sequence coverage.
[3]The MASCOT score.
[4]The number of mass values matched.
[5]Theoretical Mr and pI values based on the UniProtKB/NCBI databases.
[6]Experimental Mr and pI values computed for each identified protein spot based on the standard 2-D markers.
[7]Subcellular localization according to UniProtKB database (http://www.uniprot.org).

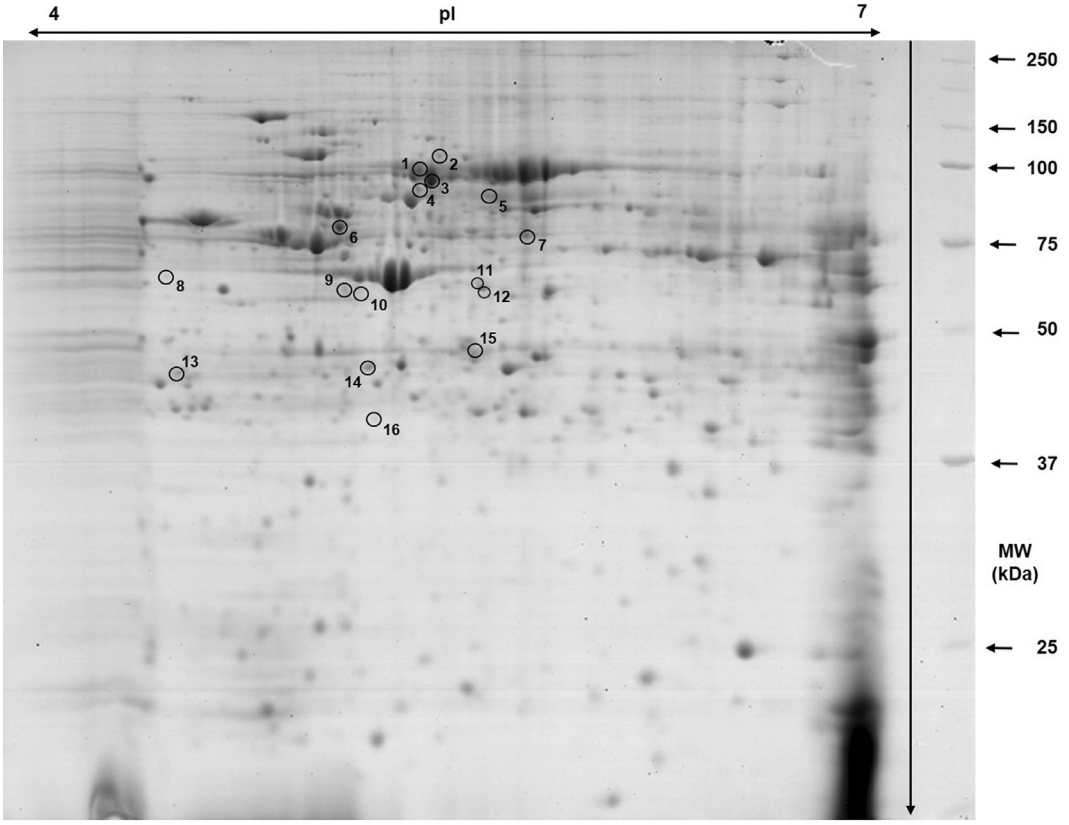


**Figure 1.** Representative 2-D gel image displaying differentially expressed proteins found in the liver of broiler chickens after in ovo injection of synbiotic − *Lactobacillus plantarum* with RFO. Spot numbers correspond to those in Table 2. Abbreviation: RFO, raffinose family oligosaccharides.

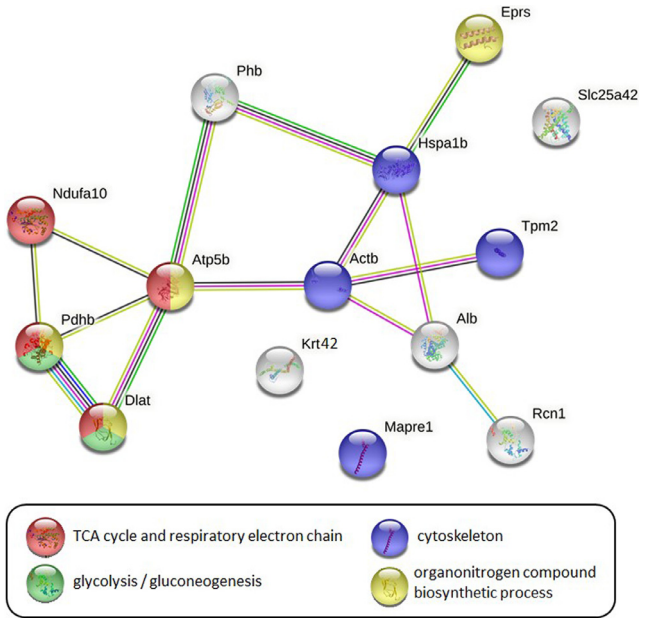


**Figure 2.** String v11 protein-protein interaction network based on input of significantly altered chicken liver proteins after in ovo injection of synbiotic − *Lactobacillus plantarum* with RFO. Each colored nodes represents included protein. Abbreviation: RFO, raffinose family oligosaccharides.

the endoplasmic reticulum (**ER**) (Table 2). These results were further supported by the analysis of differentially expressed hepatic proteins based on their biological process classification, as the majority of proteins were found to be involved in metabolic processes and cytoskeleton organization (Table 2). To identify the liver protein networks that were most affected in response to in ovo synbiotic delivery, we employed the STRING v11 tool. The STRING analysis showed that the affected protein networks included the proteins involved in the TCA cycle and respiratory electron chain, glycolysis/gluconeogenesis, and organonitrogen compound biosynthesis, and cytoskeleton proteins. The enrichment results are shown in Figure 2.

## DISCUSSION

The previous research on the use of in ovo stimulation on d 12 of egg incubation in chickens has shown that the administration of the synbiotic significantly affects the production and blood parameters, meat quality, structure and development of immune tissues, intestinal histology and molecular changes at the mRNA level (Siwek et al., 2018). Our recent study demonstrated that in ovo stimulation with *Lactobacillus*-based synbiotics induced changes in gene expression involved in regulating energy metabolism in the pectoral muscle of broiler chicken (Dunisławska et al., 2020). These data revealed that such early intervention plays a crucial role in stimulating the oxidation of fatty acids through AMPK activation, and it also decreases the activity of mechanisms involved in intracellular lipid accumulation in muscle tissue in 7-day-old birds. Given that liver and

skeletal muscle play a significant role in regulating whole body energy metabolism Our research aimed to expand the existing results and investigate whether in ovo stimulation with *L. plantarum* combined with RFO has the potential to induce changes in the hepatic proteome of adult broiler chickens. Our previous transcriptomic study, which was performed on the same group of animals, revealed that the most abundantly represented group of liver genes activated in response to in ovo injection of *Lactobacillus* synbiotic injection were involved in the metabolic pathways (Dunislawska et al., 2019). The results of the current proteomic research support these findings as the vast majority of the differentially expressed liver proteins were also associated with the regulation of energy metabolism and metabolic homeostasis. Among them, 2 proteins, identified as PDCE2 and PDHE1-B belonging to pyruvate dehydrogenase complex (**PDC**), were found to be overexpressed in the experimental group. PDC is a mitochondrial multienzyme complex that plays a central role in cellular energy metabolism as it catalyzes the overall conversion of pyruvate, coenzyme A (CoA), and $NAD^+$ into acetyl-CoA, NADH, and $CO_2$, thereby interconnecting the pathways of glycolysis, gluconeogenesis, and fatty acid oxidation to the citric acid cycle (**CAC**) (Zhang et al., 2014). Our results showed that in ovo synbiotic injection significantly increased the expression of the subunit beta of the pyruvate dehydrogenase E1 component (PDHE1-B), which is known as a rate-limiting enzyme of the whole PDC (Li et al., 2017). It should also be emphasized that the PDC activity was reported to be high in the well-fed state and low in the fasting state, when glucose synthesis is required (Zhang et al., 2014). Upregulation of both PDCE2 and PDHE1-B proteins, which was observed in this study, might be explained by the increased intestinal production of short-chain fatty acids (**SCFAs**) after in ovo stimulation with *Lactobacillus* synbiotic and its subsequent transfer into the liver from the gut through the hepatic portal vein, where they are metabolized by hepatocytes (Schönfeld and Wojtczak, 2016). Although cecal and colonic SCFA concentrations were not measured in the current study, it was previously demonstrated that in broiler chickens administration of a synbiotic (Ding et al., 2019) or probiotic (Peng et al., 2016) led to an increase in cecal SCFA content that constitutes an important substrate of energy metabolism. Our findings are in agreement with a previous study (Patel et al., 1983), in which rodent-derived liver cells treated with 1 mM propionate displayed increased mitochondrial PDC activity whereas at 0.5 mM the PDC was found to be inactivated. In general, in hepatocytes, an increase in the NADH/$NAD^+$, acetyl CoA/CoA, or ATP/ADP ratio suppresses the activity of the mitochondrial matrix enzymes, including the PDC (Schönfeld and Wojtczak, 2016). Therefore, the opposite trend of PDC activity observed by Patel et al. (1983) might be explained by the protecting effect of propionate against its inactivation by the pyruvate dehydrogenase kinase which, in turn, is triggered by high cellular ATP levels. The results of the current study seem to support the aforementioned findings, as we observed enhanced expression of ATP-synthase subunit beta (**ATP5B**), a protein that plays a central role in controlling mitochondrial ATP synthesis, in the liver of broiler chickens in response to in ovo synbiotic injection. Previously, Wang et al. (2014) showed that upregulation of ATP5B increased the intracellular and extracellular content of ATP in primary cultures of mouse hepatocytes. This effect was also accompanied by increased abundance of SLC25A42, a mitochondrial protein known for its role as transporter of CoA, an essential cofactor in pyruvate oxidation in CAC (Kunji et al., 2020). In addition, the present study showed that the expression of glutamate dehydrogenase 1 (**GDH 1**), an enzyme that catalyzes the reversible conversion of glutamate to $\alpha$-ketoglutarate and ammonia, was significantly decreased in the experimental group. As demonstrated in a previous study (Plaitakis et al., 2017), when the cellular level of ATP is high, the conversion of glutamate to $\alpha$-ketoglutarate and other CAC intermediates is strongly limited, which might result in a significantly decreased expression of liver GDH 1, as observed in the current work. Our further analysis also confirmed that in ovo treatment with *Lactobacillus*-based synbiotic caused an increase in the expression of hepatic NDUFA 10 protein, one of the subunits of NADH dehydrogenase, which is the largest enzyme of the oxidative phosphorylation system (Hoefs et al., 2011). Together, our results suggest that in ovo-delivered synbiotics might accelerate the major energy-yielding metabolic pathways in the liver of adult broilers as reflected by an increased expression of proteins involved in CAC, electron transport chain, and ATP synthesis.

Furthermore, the present study demonstrated that the expression of heat shock protein 70 (**HSP70**) was significantly downregulated in the livers of birds from the experimental group when compared to the control group. In a recent study, Jiang et al. (2019) observed a similar pattern of HSP70 protein expression in the liver of broiler chickens fed a diet supplemented with the synbiotic product (PoultryStar me, BIOMIN America Inc., San Antonio, TX) and reared under cyclic heat stress. Apart from its well-known role as a molecular chaperonin, HSP70 has been shown to promote hepatic lipogenesis. A previous study by Zhang et al. (2018) showed that HSP70 was significantly increased in the livers of obese mice which in turn enhanced hepatic total cholesterol and triglyceride synthesis, with a concomitant upregulation of lipogenic genes. In addition, our data revealed that in ovo synbiotic stimulation resulted in a decreased expression of EPRS1, a multifunctional protein that primarily catalyzes attachment of the cognate amino acid to corresponding tRNA (Son et al., 2013). However, a recent study by Arif et al. (2017) provided additional evidence that EPRS phosphorylation also contributes to lipid accumulation by inhibiting catabolic reactions, such as lipolysis and fatty acid oxidation, in transgenic mice. Therefore, our data seem to support the general conclusion that SCFAs are implicated in the activation of hepatic mechanisms mainly via G-protein coupled

receptors—FFAR3—leading to improved lipid metabolism (Shimizu et al., 2019), as substantial downregulation of HSP70 and EPRS1 proteins was observed in the synbiotic-treated group.

In the current study, in ovo treatment with *Lactobacillus*-based synbiotic caused significant overexpression of liver proteins involved in cytoskeleton organization. These proteins were found to belong to the 3 different protein structures forming the cytoskeletal network, namely microtubules (MAPRE1), microfilaments (ACTB, TPM2), and intermediate filaments (CK-42). In contrast, other studies performed on growing pigs fed diets containing prebiotic fructans (chicory inulin extracts or dried chicory root) demonstrated different patterns of liver cytoskeletal protein expression (Herosimczyk et al., 2017; Lepczyński et al., 2017). As reviewed by Doctor and Nichols (2004), cytoskeletal proteins are largely involved in maintaining intracellular transport and several signaling cascades, thus modulating the metabolic function of hepatocytes. However, the fundamental molecular mechanisms that regulate the expression of cytoskeletal proteins in the chicken liver in response to in ovo synbiotic stimulation is difficult to explain, which warrants further investigations.

There exists a large body of evidence that microbiota itself as well as their primary fermentation end-products, including SCFAs, may have an impact on mitochondrial functions (Mottawea et al., 2016; Clark and Mach, 2017). This is further supported by the results of the present study as we observed in the subcellular distribution analysis that nearly half of the proteins affected in response to in ovo synbiotic administration were those residing within the mitochondria of hepatocytes. In addition to their central role in energy metabolism, mitochondria along with ER participate in the regulation of intracellular calcium homeostasis. This is also supported by the results of this study, as reticulocalbin-1 (**RCN1**), a protein involved in the regulation of calcium-dependent activities in the ER lumen, was found to be overexpressed in the livers of birds from the experimental group (Liu et al., 2018). Unfortunately, the definitive physiological roles of RCN1 in the liver are poorly understood and need to be elucidated. Nevertheless, an increased expression of RCN1 may confirm the positive effect of in ovo synbiotic treatment on the liver, as this protein is known as a chaperonin with documented roles in preventing protein aggregation and ensuring proper function of ER (Liu et al., 2018).

In summary, the results of the present study indicate that in ovo stimulation with *Lactobacillus*-based synbiotic might have a profound impact on mitochondrial functions as the vast majority of significantly altered proteins were found to reside within the hepatic mitochondria. Based on the differential analysis of the aforementioned proteins, we conclude that in ovo synbiotic treatment had the potential to accelerate the major energy-yielding metabolic pathways in the liver of adult broilers, which was reflected by an increased expression of proteins involved in CAC, electron transport chain, and ATP synthesis. Furthermore, a tendency for decreased expression of HSP70 and EPRS1 proteins found in the experimental group may support the general idea that SCFAs may downregulate lipogenic pathways resulting in decreased hepatic lipid accumulation. The results of current study can be considered preliminary and they require further confirmation using more sophisticated proteomic techniques. Therefore, our research inputs will be extended to other methods such as UHPLC-ESI-QTOF MS system to reveal many more hepatic proteins that may be altered in response to in ovo stimulation with *Lactobacillus*-based synbiotic.

## ACKNOWLEDGMENTS

The research was supported by grant UMO-2017/25/N/NZ9/01822 funded by the National Science Centre in Cracow (Poland)

## DISCLOSURES

The authors no conflicts of interest to report.

## REFERENCES

Arif, A., F. Terenzi, A. A. Potdar, J. Jia, J. Sacks, A. China, D. Halawani, K. Vasu, X. Li, J. M. Brown, J. Chen, S. C. Kozma, G. Thomas, and P. L. Fox. 2017. EPRS is a critical mTORC1-S6K1 effector that influences adiposity in mice. Nature 542:357–361.

Bäckhed, F. 2011. Programming of host metabolism by the gut microbiota. Ann. Nutr. Metab. 58:44–52.

Bednarczyk, M., K. Stadnicka, I. Kozłowska, C. Abiuso, S. Tavaniello, A. Dankowiakowska, A. Sławińska, and G. Maiorano. 2016. Influence of different prebiotics and mode of their administration on broiler chicken performance. Animal 1271–1279.

Ciesiołka, D., P. Gulewicz, C. Martinez-Villaluenga, R. Pilarski, M. Bednarczyk, and K. Gulewicz. 2005. Products and biopreparations from alkaloid-rich lupin in animal nutrition and ecological agriculture. Folia Biologica (Krakow) 53:59–66.

Clark, A., and N. Mach. 2017. The crosstalk between the gut microbiota and mitochondria during exercise. Front. Physiol. 8:319.

Ding, S., Y. Wang, W. Yan, A. Li, H. Jiang, and J. Fang. 2019. Effects of Lactobacillus plantarum 15-1 and fructooligosaccharides on the response of broilers to pathogenic Escherichia coli O78 challenge. PLoS One 14:e0212079.

Doctor, R. B., and M. Nichols. 2004. The actin cytoskeleton in liver function. Principles Med. Biol. 15:49–79.

Dunislawska, A., A. Slawinska, M. Bednarczyk, and M. Siwek. 2019. Transcriptome modulation by in ovo delivered Lactobacillus synbiotics in a range of chicken tissues. Gene 698:27–33.

Dunislawska, A., A. Slawinska, and M. Siwek. 2020. Hepatic DNA methylation in response to early stimulation of microbiota with Lactobacillus synbiotics in broiler chickens. Genes (Basel) 11:579.

Dunislawska, A., M. Siwek, A. Slawinska, A. Lepczynski, A. Herosimczyk, P. A. Kolodziejski, and M. Bednarczyk. 2020. Metabolic gene expression in the muscle and blood parameters of broiler chickens stimulated in ovo with synbiotics. Animals (Basel). 10:687.

Dunislawska, A., A. Slawinska, K. Stadnicka, M. Bednarczyk, P. Gulewicz, D. Jozefiak, and M. Siwek. 2017. Synbiotics for broiler chickens—in vitro design and evaluation of the influence on host and selected microbiota populations following in ovo delivery (BAWilson, Ed.). PLoS One 12:e0168587.

Fuller, R. 1989. Probiotics in man and animals. J. Appl. Bacteriol. 66:365–378.

Gibson, G. R., and M. B. Roberfroid. 1995. Dietary modulation of the human colonic microbiota: introducing the concept of prebiotics. J. Nutr. 125:1401–1412.

Hajati, H., and M. Rezaei. 2010. The application of prebiotics in poultry production. Int. J. Poult. Sci. 9:298–304.

Herosimczyk, A., A. Lepczyński, M. Ożgo, M. Barszcz, E. Jaszczuk-Kubiak, M. Pierzchała, A. Tuśnio, and J. Skomiał. 2017. Hepatic proteome changes induced by dietary supplementation with two levels of native chicory inulin in young pigs. Livest. Sci. 203:54–62.

Herosimczyk, A., A. Lepczynski, M. Ozgo, M. Barszcz, M. Marynowska, A. Tusnio, M. Taciak, A. Markulen, and J. Skomial. 2018. Proteome changes in ileal mucosa of young pigs resulting from different levels of native chicory inulin in the diet. J. Anim. Feed Sci. 27:229–237.

Herosimczyk, A., A. Lepczyński, M. Ozgo, A. Tuśnio, M. Taciak, and M. Barszcz. 2020. Effect of dietary inclusion of 1% or 3% of native chicory inulin on the large intestinal mucosa proteome of growing pigs. Animal 14:1647–1658.

Hoefs, S. J. G., F. J. Van Spronsen, E. W. H. Lenssen, L. G. Nijtmans, R. J. Rodenburg, J. A. M. Smeitink, and L. P. Van Den Heuvel. 2011. NDUFA10 mutations cause complex i deficiency in a patient with Leigh disease. Eur. J. Hum. Genet. 19:270–274.

Jiang, S., A. A. Mohammed, J. A. Jacobs, T. A. Cramer, and H. W. Cheng. 2019. Effect of synbiotics on thyroid hormones, intestinal histomorphology, and heat shock protein 70 expression in broiler chickens reared under cyclic heat stress. Poult. Sci. 99:142–150.

Kunji, E. R. S., M. S. King, J. J. Ruprecht, and C. Thangaratnarajah. 2020. The SLC25 carrier family: important transport proteins in mitochondrial physiology and pathology. Physiology 35:302–327.

Lepczyński, A., A. Herosimczyk, M. Ożgo, M. Marynowska, M. Pawlikowska, M. Barszcz, M. Taciak, and J. Skomiał. 2017. Dietary chicory root and chicory inulin trigger changes in energetic metabolism, stress prevention and cytoskeletal proteins in the liver of growing pigs – a proteomic study. J. Anim. Physiol. Anim. Nutr. (Berl). 101:e225–e236.

Li, L., M. Peng, C. Ge, L. Yu, and H. Ma. 2017. (-)-Hydroxycitric acid reduced lipid droplets accumulation via decreasing acetyl-coa supply and accelerating energy metabolism in cultured primary chicken hepatocytes. Cell. Physiol. Biochem. 43:812–831.

Liu, X., N. Zhang, D. Wang, D. Zhu, Q. Yuan, X. Zhang, L. Qian, H. Niu, Y. Lu, G. Ren, K. Tian, and H. Yuan. 2018. Downregulation of reticulocalbin-1 differentially facilitates apoptosis and necroptosis in human prostate cancer cells. Cancer Sci 109:1147–1157.

Mottawea, W., C. K. Chiang, M. Mühlbauer, A. E. Starr, J. Butcher, T. Abujamel, S. A. Deeke, A. Brandel, H. Zhou, S. Shokralla, M. Hajibabaei, R. Singleton, E. I. Benchimol, C. Jobin, D. R. Mack, D. Figeys, and A. Stintzi. 2016. Altered intestinal microbiota-host mitochondria crosstalk in new onset Crohn's disease. Nat. Commun. 7:13419.

Ozgo, M., A. Lepczynski, P. Robak, A. Herosimczyk, and M. Marynowska. 2019. The current proteomic landscape of the porcine liver. J. Physiol. Pharmacol. 70:369–387.

Patel, T. B., M. S. DeBuysere, and M. S. Olson. 1983. The effect of propionate on the regulation of the pyruvate dehydrogenase complex in the rat liver. Arch. Biochem. Biophys. 220:405–414.

Patterson, J. A., and K. M. Burkholder. 2003. Application of prebiotics and probiotics in poultry production. Poult. Sci. 82:627–631.

Peng, Q., X. F. Zeng, J. L. Zhu, S. Wang, X. T. Liu, C. L. Hou, P. A. Thacker, and S. Y. Qiao. 2016. Effects of dietary Lactobacillus plantarum B1 on growth performance, intestinal microbiota, and short chain fatty acid profiles in broiler chickens. Poult. Sci. 95:893–900.

Pink, M., N. Verma, A. W. Rettenmeier, and S. Schmitz-Spanke. 2010. CBB staining protocol with higher sensitivity and mass spectrometric compatibility. Electrophoresis 31:593–598.

Plaitakis, A., E. Kalef-Ezra, D. Kotzamani, I. Zaganas, and C. Spanaki. 2017. The glutamate dehydrogenase pathway and its roles in cell and tissue biology in health and disease. Biology (Basel) 6:11.

Schönfeld, P., and L. Wojtczak. 2016. Short- and medium-chain fatty acids in energy metabolism: the cellular perspective. J. Lipid Res. 57:943–954.

Shimizu, H., Y. Masujima, C. Ushiroda, R. Mizushima, S. Taira, R. Ohue-Kitano, and I. Kimura. 2019. Dietary short-chain fatty acid intake improves the hepatic metabolic condition via FFAR3. Sci Rep 9:16574.

Sikorska, M., M. Siwek, A. Slawinska, and A. Dunislawska. 2021. miRNA profiling in the chicken liver under the influence of early microbiota stimulation with probiotic, prebiotic, and synbiotic. Genes 12:685.

Siwek, M., A. Slawinska, K. Stadnicka, J. Bogucka, A. Dunislawska, and M. Bednarczyk. 2018. Prebiotics and synbiotics – in ovo delivery for improved lifespan condition in chicken. BMC Vet. Res. 14:402.

Son, J., E. H. Lee, M. Park, J. H. Kim, J. Kim, S. Kim, Y. H. Jeon, and K. Y. Hwang. 2013. Conformational changes in human prolyl-tRNA synthetase upon binding of the substrates proline and ATP and the inhibitor halofuginone. Acta Crystallogr. Sect. D Biol. Crystallogr. 69:2136–2145.

Szabo, G. 2015. Gut-liver axis in alcoholic liver disease. Gastroenterology 148:30–36.

Szklarczyk, D., A. Franceschini, M. Kuhn, M. Simonovic, A. Roth, P. Minguez, T. Doerks, M. Stark, J. Muller, P. Bork, L. J. Jensen, and C. Von Mering. 2011. The STRING database in 2011: functional interaction networks of proteins, globally integrated and scored. Nucleic Acids Res 47:D607–D613.

Racanelli, V, and B. Rehermann. 2006. The liver as an immunological organ. Hepatology 43:S54–S62.

Tavaniello, S., R. Mucci, K. Stadnicka, O. Acaye, M. Bednarczyk, and G. Maiorano. 2019. Effect of in ovo administration of different synbiotics on carcass and meat quality traits in broiler chickens. Poult. Sci. 98:464–472.

Tlaskalová-Hogenová, H., R. Štěpánková, H. Kozáková, T. Hudcovic, L. Vannucci, L. Tučková, P. Rossmann, T. Hrnčíř, M. Kverka, Z. Zákostelská, K. Klimešová, J. Přibylová, J. Bártová, D. Sanchez, P. Fundová, D. Borovská, D. Šrůtková, Z. Zídek, M. Schwarzer, P. Drastich, and D. P. Funda. 2011. The role of gut microbiota (commensal bacteria) and the mucosal barrier in the pathogenesis of inflammatory and autoimmune diseases and cancer: contribution of germ-free and gnotobiotic animal models of human diseases. Cell. Mol. Immunol. 8:110–120.

Tripathi, A., J. Debelius, D. A. Brenner, M. Karin, R. Loomba, B. Schnabl, and R. Knight. 2018. The gut-liver axis and the intersection with the microbiome. Nat. Rev. Gastroenterol. Hepatol 15:397–411.

Villaluenga, C. M., M. Wardeńska, R. Pilarski, M. Bednarczyk, and K. Gulewicz. 2004. Utilization of the chicken embryo model for assessment of biological activity of different oligosaccharides. Folia Biol. (Krakow). 52:135–142.

Wang, C., Z. Chen, S. Li, Y. Zhang, S. Jia, J. Li, Y. Chi, Y. Miao, Y. Guan, and J. Yang. 2014. Hepatic overexpression of ATP synthase $\beta$ subunit activates PI3K/Akt pathway to ameliorate hyperglycemia of diabetic mice. Diabetes 63:947–959.

Zhang, J., N. Fan, and Y. Peng. 2018. Heat shock protein 70 promotes lipogenesis in HepG2 cells. Lipids Health Dis 17:73.

Zhang, S., M. W. Hulver, R. P. McMillan, M. A. Cline, and E. R. Gilbert. 2014. The pivotal role of pyruvate dehydrogenase kinases in metabolic flexibility. Nutr. Metab. 11:10.